Transcriptional Control of the Lateral-Flagellar Genes of *Bradyrhizobium diazoefficiens*

Elías J. Mongiardini, J. Ignacio Quelas, Carolina Dardis, M. Julia Althabegoiti, Aníbal R. Lodeiro

Instituto de Biotecnología y Biología Molecular, Facultad de Ciencias Exactas, Universidad Nacional de La Plata y CCT-La Plata, CONICET, La Plata, Argentina

ABSTRACT *Bradyrhizobium diazoefficiens*, a soybean N_2-fixing symbiont, possesses a dual flagellar system comprising a constitutive subpolar flagellum and inducible lateral flagella. Here, we analyzed the genomic organization and biosynthetic regulation of the lateral-flagellar genes. We found that these genes are located in a single genomic cluster, organized in two monocistronic transcriptional units and three operons, one possibly containing an internal transcription start site. Among the monocistronic units is blr6846, homologous to the class IB master regulators of flagellum synthesis in *Brucella melitensis* and *Ensifer meliloti* and required for the expression of all the lateral-flagellar genes except *lafA2*, whose locus encodes a single lateral flagellin. We therefore named blr6846 *lafR* (lateral-flagellar regulator). Despite its similarity to two-component response regulators and its possession of a phosphorylatable Asp residue, *lafR* behaved as an orphan response regulator by not requiring phosphorylation at this site. Among the genes induced by *lafR* is *flbT_L*, a class III regulator. We observed different requirements for FlbT_L in the synthesis of each flagellin subunit. Although the accumulation of *lafA1*, but not *lafA2*, transcripts required FlbT_L, the production of both flagellin polypeptides required FlbT_L. Moreover, the regulation cascade of this lateral-flagellar regulon appeared to be not as strictly ordered as those found in other bacterial species.

IMPORTANCE Bacterial motility seems essential for the free-living style in the environment, and therefore these microorganisms allocate a great deal of their energetic resources to the biosynthesis and functioning of flagella. Despite energetic costs, some bacterial species possess dual flagellar systems, one of which is a primary system normally polar or subpolar, and the other is a secondary, lateral system that is produced only under special circumstances. *Bradyrhizobium diazoefficiens*, an N_2-fixing symbiont of soybean plants, possesses dual flagellar systems, including the lateral system that contributes to swimming in wet soil and competition for nodulation and is expressed under high energy availability, as well as under requirement for high torque by the flagella. The structural organization and transcriptional regulation of the 41 genes that comprise this secondary flagellar system seem adapted to adjust bacterial energy expenditures for motility to the soil's environmental dynamics.

KEYWORDS *Bradyrhizobium*, flagella, expression, *lafR*, *flbT*, FlbT, LafR

Flagellum-driven swimming motility—a characteristic trait of many bacterial species—is essential for the colonization of diverse niches in environments such as seas, freshwaters, sediments, soils, and the organs of plant or animal hosts. This form of bacterial locomotion requires the propulsion provided by flagella, as well as a guidance system mediated by chemotaxis (1).

Flagella are complex organelles formed by three main structures: a basal body that anchors the flagellum to the cell envelope, a filament that projects out from the cell

often with a length greater than the cell body itself, and a hook that connects the basal body to the filament (see Fig. S1 in the supplemental material). The basal body, the most complex of these substructures, is responsible for two critical tasks: exporting the hook and filament proteins synthesized in the cytoplasm toward the extracellular space (2, 3) and providing the rotational motion of the flagella (4–6). For the first task, an export apparatus is embedded in the inner cell membrane ending in a rod that crosses the cell envelope and delivers the hook and filament polypeptides. Because the rod's internal channel is narrow, the polypeptides must pass through in a partially unfolded state, whose conformation is stabilized by specific chaperones through proton motive force and ATP hydrolysis as energy sources. For the second task, the basal body contains the flagellar motor, composed of a stator in the inner cell membrane and a rotor formed by a ring of several protein subunits that rotates inside the stator by the proton or sodium ion motive force. In turn, the hook and the filament are formed by the polymerization of thousands of monomers of structural proteins and are held together by specific hook-filament junctions (7, 8). The hook is a flexible connector that transmits motor rotation in the form of waves to the flagellar filament, whose extension in turn rotates while undulating like an Archimedean screw to drag or thrust the cell in an aqueous medium, depending on whether the flagellum is ahead or behind the cell, respectively (9). In Gram-negative bacteria, the whole structure passes through the inner membrane, the peptidoglycan layer, and the outer membrane, with each layer containing rings that behave like bushings. The >40 genes that encode the basal body, the hook, the filament, the rings, and the auxiliary and regulatory proteins lie in a limited number of operons that, together with the chemotaxis genes, comprise the flagellar regulon.

The synthesis and assemblage of the bacterial flagellum require a substantial organization in order to ensure that all the major structures are completed sequentially from the membrane-associated elements to the extracellular components (10, 11). Thus, depending on the species, the regulation of flagellum biosynthesis comprises three or four principal steps, whose stages have been carefully studied in model systems such as *Caulobacter crescentus*, *Ensifer meliloti*, *Escherichia coli*, *Pseudomonas* spp., *Salmonella enterica*, and *Vibrio* spp., among others (12–14). In general, a master regulator (class I) induces the expression of several flagellar operons (class II) that encode the basal body, the hook and hook-related proteins, and a regulator of the synthesis of the filament monomers or flagellins. Therefore, these flagellins (class III) are synthesized in the final step, with the basal body and the hook already in position. This strategy ensures that no energy is wasted on flagellin synthesis and export before these proteins are required (10, 13).

The rotation of the flagellar motor defines whether a bacterium swims in a given direction or erratically. In general, when the flagella rotate in a single direction, the bacteria swim in linear runs, whose stretches are interrupted when flagellar rotation switches direction or stops (15–18). The frequency at which these changes in direction occur are governed by the chemotaxis system in response to chemical stimuli (i.e., attractant or repellent gradients) present in the medium (18). As with the flagellar genes, the chemotaxis loci are often arranged in operons under control by the same regulators that govern the synthesis of flagellins and therefore are also grouped in class III of the flagellar regulon (13).

Bradyrhizobium diazoefficiens, the soybean N_2-fixing symbiont, is a soil alphaproteobacterium that possesses two different flagellar systems with independent evolutionary origins (19, 20). One of these systems involves a subpolar flagellum closely related to the one in *C. crescentus*, while the other is characterized by lateral flagella similar to those in *E. meliloti* (20). The expression of each flagellar system is also different. The subpolar system seems constitutive within a range of conditions; by contrast, the expression of the lateral system requires arabinose as a carbon source or viscosity in the culture medium or the presence of obstacles in the swimming path (20–22). Hence, growth in liquid medium with mannitol as the carbon source does not permit the expression of the lateral flagella. Transcriptomic studies have also indicated that

conditions of microoxia (23) or iron deficiency (24) prevent the expression of lateral-flagellar genes, whereas permanent exposure to moderate oxidative stress induces these loci (25). In the example of *Ensifer meliloti* and its close relative *Brucella melitensis*, flagellar expression is also under strict control by specific nutritional, physiological, and population-size requirements (26–29).

In contrast to other species having dual flagellar systems that use one exclusively for swimming in a liquid medium and the other only for swarming on surfaces, both flagellar systems of *B. diazoefficiens* may be utilized together in liquid medium and interact to produce an emergent swimming performance that allows the bacterium to continually swim alongside solid surfaces (20). Only the subpolar system, however, responds to chemotactic stimuli, whereas only the lateral system contributes to swimming in viscous-agar-containing medium (20). Although neither of these flagellar systems is required for the nodulation of soybean plants (30), bacterial motility might be essential for nodule occupation in competition against populations of compatible rhizobia in the soil (31). In earlier work, we obtained a derivative of *B. diazoefficiens* USDA 110 with higher motility by *in vitro* selection (21). The inoculation of this derivative on experimental soybean crops planted in soils with dense soybean-nodulating competitor populations resulted in an enhanced nodule occupation by the derivative and promoted a higher soybean grain yield (21, 31). Further studies indicated that the lateral-flagellar system of this derivative became derepressed upon culture in liquid medium with mannitol as the carbon and energy source (21, 22). Therefore, the control of lateral-flagellar synthesis in this species should take into account the cell's needs on the basis of the environmental conditions in order to coordinate the activity of both flagellar systems, which would appear to be essential for the symbiotic interaction with soybean plants. To better understand the regulation of these genetically controlled functions, in the study reported here, we investigated the organization and transcriptional control of the lateral-flagellar genes of *B. diazoefficiens* USDA 110.

RESULTS

Identification and characterization of *lafR*, the master regulator of lateral-flagellar synthesis in *B. diazoefficiens* USDA 110. In *E. meliloti*, flagellar expression is controlled by a regulatory circuit composed of the LuxR-type master regulators VisNR and the OmpR-like transcriptional activator Rem (28). In a similar fashion, the LuxR-type VjbR and the OmpR-like FtcR are master regulators of flagellar expression in *B. melitensis* (32). Although the regulation circuit of neither VisNR nor VjbR is restricted to flagellar gene expression, the Rem and FtcR regulators seem to be more specific (28, 32). In addition, since the expression of *rem* and *ftcR* is regulated by VisNR and VjbR, respectively, the LuxR-type components were classified as class IA, whereas the OmpR-like components were considered class IB (28, 32). Within the complete genomic sequence of *B. diazoefficiens* USDA 110 (33), we could not find homologs to *visNR* or *vjbR*, but the locus tag blr6846 (Ga0076376_112362 in the reannotation at the IMG database)—located near the cluster of genes that encode the lateral flagella in *B. diazoefficiens*—encodes a predicted OmpR-like transcriptional-response regulator of 256 residues homologous to Rem and FtcR and harboring the typical receiver and helix-turn-helix DNA-binding domains (see Fig. S2A in the supplemental material). The high similarity among these three OmpR-like transcriptional-response regulators, as well as the position of blr6846 with respect to the lateral flagellar gene cluster, led us to suspect that blr6846 might be a master regulator of the synthesis of the lateral flagella in *B. diazoefficiens*. This suspicion was reinforced by the observation that the expression of blr6846 is dependent on the carbon source in a manner similar to that of the production of the lateral flagellins LafA1 and LafA2, since blr6846 is expressed in arabinose-grown cultures at substantially higher levels than in mannitol-containing cultures (Fig. 1A and B). In addition, a mutant harboring a kanamycin (Km)-resistant cassette inserted at base 7543291 in the middle of the coding sequence of blr6846, thus disrupting the connection between the receiver and helix-turn-helix DNA-binding domains (see Fig. S2B in the supplemental material), was found to lack lateral flagellins
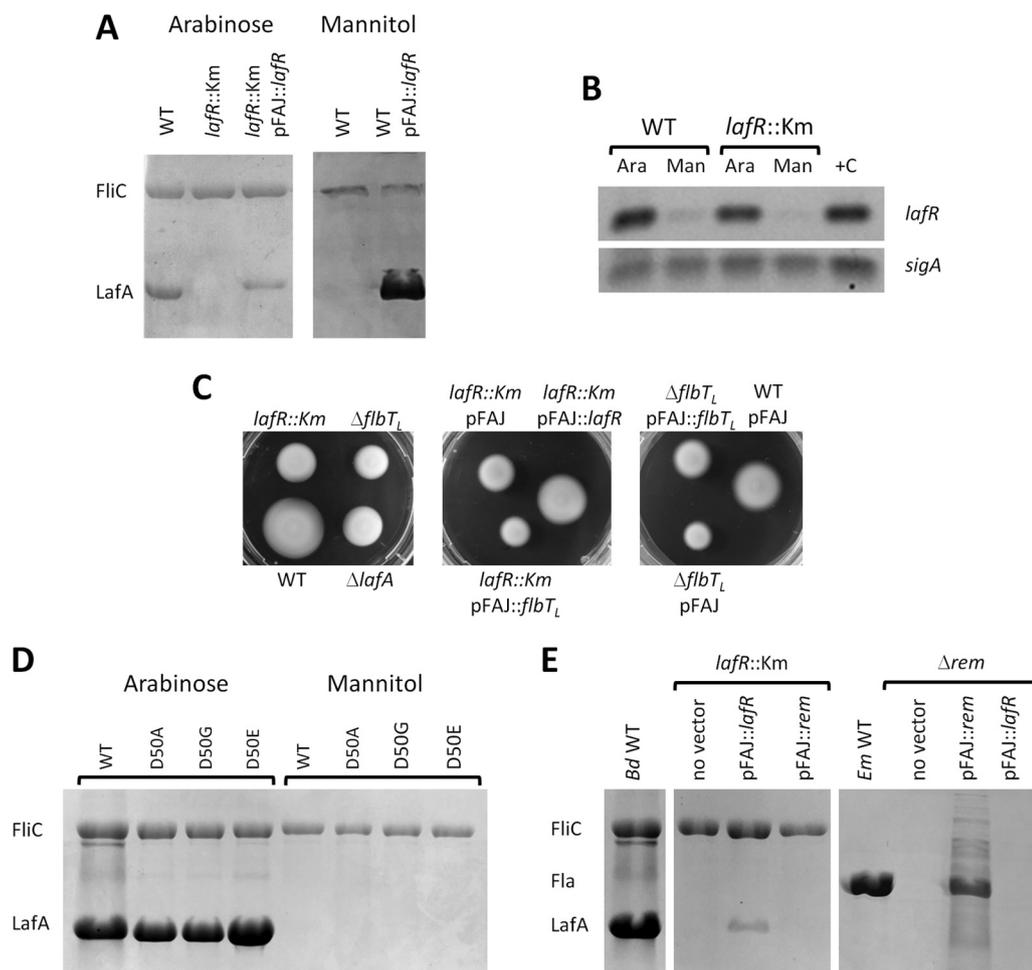
FIG 1 Control of flagellin expression and motility by *lafR* in bacteria grown in liquid HMY with arabinose (Ara) or mannitol (Man) as a carbon source. (A) SDS-PAGE of extracellular *B. diazoefficiens* proteins of the subpolar flagellins (FliC, upper bands) and lateral flagellins (LafA, lower bands) in the wild-type (WT) and the *lafR*::Km extracts alone or in extracts from the WT and the *lafR*::Km strains complemented with a WT copy of *lafR* under the direction of the *nptII* promoter (pFAJ::*lafR*). (B) Agarose gel of RNA retrotranscripts amplified by RT-PCR of *lafR* in the WT or the *lafR*::Km mutant with the primers indicated in Fig. S2B and listed in Table S2 in the supplemental material compared to *sigA* as constitutive reference gene. A PCR from genomic DNA was performed as a positive control (+C). (C) Swimming motility in 0.3% (wt/vol) agar-containing AG medium. Left panel: wild type compared to *lafR*::Km, Δ*flbT_L*, and Δ*lafA* mutants, the last one lacking lateral flagellins. Center panel: complementation of motility in the *lafR*::Km mutant with the pFAJ::*lafR* plasmid in comparison to the *lafR*::Km mutant carrying empty vector (pFAJ) or *lafR*::Km mutant carrying pFAJ::*flbT_L*. Right panel: complementation of motility in the Δ*flbT_L* mutant with the pFAJ::*flbT_L* plasmid in comparison with Δ*flbT_L* mutant carrying the empty vector (pFAJ). The results of all the complementations may be compared to the motility of the WT carrying the empty vector (WT pFAJ, right). (D) SDS-PAGE of *B. diazoefficiens* extracellular proteins—the subpolar flagellins (FliC, upper bands) and lateral flagellins (LafA, lower bands)—in the wild type and *lafR* point mutants D50A (with the Asp50 residue replaced by Ala), D50G (with Asp50 replaced by Gly), and D50E (with Asp50 replaced by Glu). (E) Composite SDS-PAGE of the subpolar (FliC, upper bands) and lateral (LafA, lower bands) flagellins of *B. diazoefficiens* or the FlaA-D flagellins of *E. meliloti* (Fla, middle bands). The flagellins are from *B. diazoefficiens* (*Bd*) wild-type and *lafR*::Km mutant either alone or complemented with pFAJ::*lafR* or with a wild-type copy of *rem* under the *nptII* promoter (pFAJ::*rem*), wild-type *E. meliloti* (*Em* WT), and the *E. meliloti rem* mutant (Δ*rem*) either alone or complemented with pFAJ::*rem* or pFAJ::*lafR*. All the bacteria were grown on HMY with arabinose as the carbon source. The gels were run simultaneously in the same equipment.

even when grown with arabinose as the carbon source (Fig. 1A). The production of the lateral flagellins was restored after introducing a wild-type (WT) copy of blr6846 in the pFAJ1708 replicative plasmid, indicating that the defective phenotype resulted from the disruption of the coding sequence of blr6846. In addition, the lateral flagellin production was restored in the wild-type strain grown with mannitol when blr6846 was expressed constitutively from the replicative plasmid (Fig. 1A), demonstrating that the expression of blr6846 was sufficient to produce the lateral flagellins under this condition. However, the polypeptide levels of LafA relative to those of FliC were variable in

the complemented strains among the different experiments. Since pFAJ1708 is stable in *B. diazoefficiens*, we have no explanation for the observed instability in LafA recovery, which nevertheless does not rule out the conclusions that the *lafR*::Km mutation may be complemented in *trans* and that the presence of *lafR* in *trans* is sufficient for lateral flagellin synthesis in mannitol. The blr6846 mutant achieved a smaller swimming halo than the wild-type in soft agar, whose area was similar to that produced by the lateral flagellin-deficient Δ*lafA* mutant (Fig. 1C). This defect in swimming, observed in the mutants within the WT USDA 110 background, was also displayed by a blr6846 mutant in the LP 3004 background (the USDA 110 streptomycin [Sm]-resistant derivative) and by another blr6846 mutant in the LP 3008 background (the LP 3004 derivative with higher motility [data not shown]). In addition, motility of the *lafR*::Km mutant was restored by *trans* complementation with pFAJ::*lafR* (Fig. 1C), indicating that *lafR* expression was sufficient to produce functional lateral flagella. Taken together, these results corroborated that blr6846 might have roles similar to those of *rem* and *ftcR*, so that we refer to blr6846 here as *lafR* (lateral flagellum regulator) and have accordingly renamed the Km insertion mutation *lafR*::Km.

LafR as an orphan response regulator. A critical difference observed in the amino acid sequence of LafR with respect to its counterparts Rem and FtcR is the presence of an Asp residue at position 50 that is susceptible to phosphorylation as in the typical transcriptional response regulator OmpR (see Fig. S2A in the supplemental material). In contrast, Rem and FtcR possess a Glu at this position, the latter residue being larger than Asp by an additional methyl group (28, 32). Therefore, Rem and FtcR may function as though they were continually activated (32), whereas LafR might require phosphorylation for activation; this property would be consistent with the inducible nature of lateral flagella in *B. diazoefficiens*. We could not find, however, any putative histidine kinase associated with *lafR*. In order to elucidate this question, we constructed the single-substitution *lafR*(D50A), *lafR*(D50G), and *lafR*(D50E) mutants (see Table S1 in the supplemental material) in which the Asp50 residue was replaced by an Ala (without the carboxyl group of Asp), a Gly (without any residue), or a Glu (as in Rem and FtcR; see Fig. S2A in the supplemental material), respectively. Therefore, if phosphorylation of the Asp50 was required, neither *lafR*(D50A) nor *lafR*(D50G) would be activated, whereas *lafR*(D50E) would likely be constitutively active. Nevertheless, we observed the same profile of activation in all three mutants and in the wild type, i.e., the lateral flagellins were produced with arabinose but not with mannitol as the carbon source (Fig. 1D). Together, these results indicated that LafR behaves as an orphan response regulator whose activation seems not to require phosphorylation of Asp50 by a histidine kinase sensor.

The function of *lafR* cannot be replaced by *rem*. To further characterize the possible similarity between *lafR* and *rem*, we looked for possible cross-complementation of these genes in *B. diazoefficiens* and *E. meliloti* mutants. Thus, we introduced a wild-type copy of *rem* carried by pFAJ1708 into the *B. diazoefficiens lafR* mutant and, reciprocally, introduced a wild-type copy of *lafR* into the *E. meliloti rem* mutant Rm2011mTn5STM.1.08.H02 (i.e., referred to as the Δ*rem* mutant here [see Table S1 in the supplemental material]). The flagellins, however, were not observed in the cross-complemented strains (Fig. 1E). Since the controls complemented with the transcriptional regulator of the same species did produce flagellins, we concluded that either LafR or Rem are not stably expressed in *E. meliloti* or *B. diazoefficiens*, respectively, or the failure of cross-complementation in the experimental strains may be due to a lack of recognition in the interaction between the heterologous proteins and DNAs.

Operon organization in the lateral-flagellar gene cluster. The 41 lateral-flagellar genes of *B. diazoefficiens* are grouped in a single cluster, although evidence for the origin of that acquisition through horizontal gene transfer could not be found (20). In addition, the lack of chemotaxis genes in the vicinity of this cluster—in agreement with the lack of chemotactic response exerted by the lateral flagellar system (20)—suggests that this cluster might constitute the complete lateral-flagellar regulon. Through the
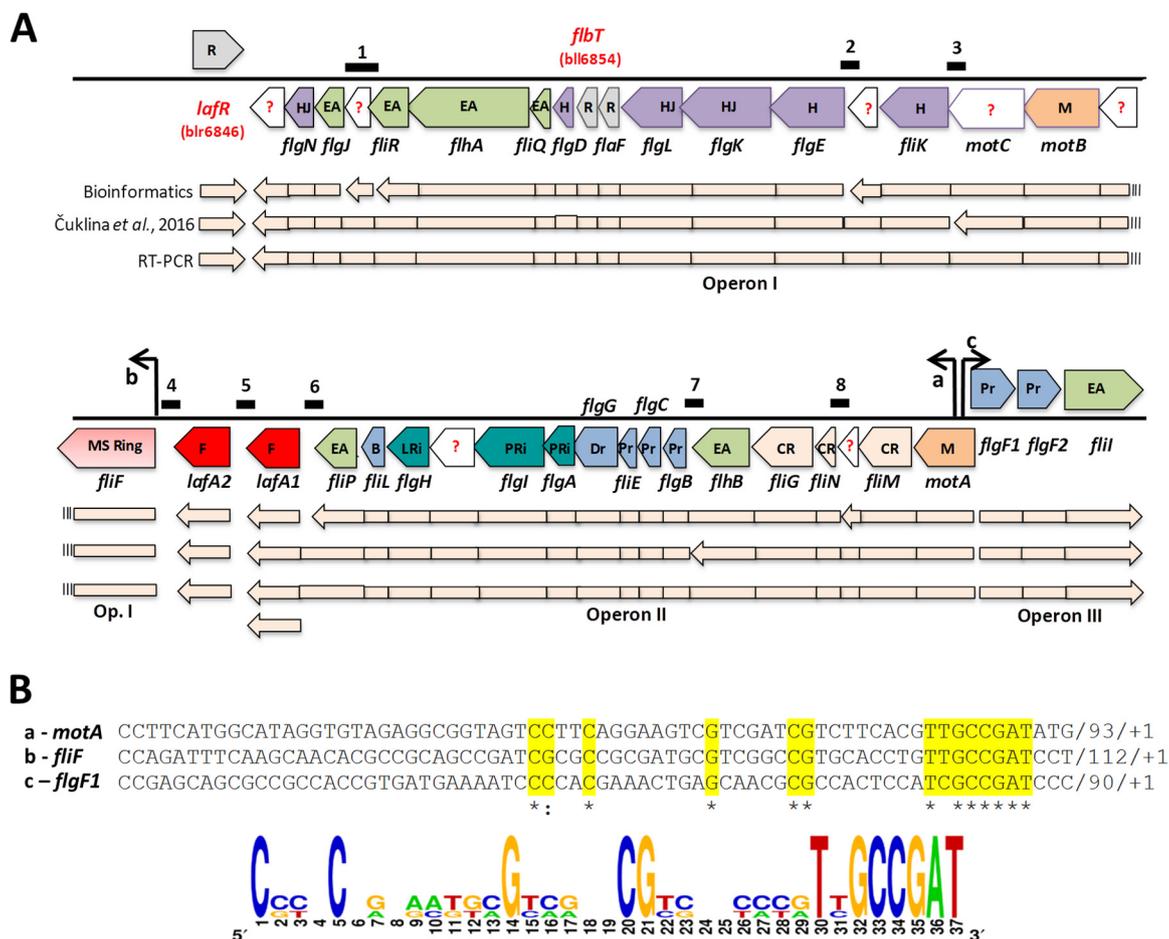
A

flbT (bll6854)

lafR (blr6846)

R | ? | HJ | EA | ? | EA | EA | EA | H | R | R | HJ | HJ | H | ? | H | ? | M | ?

flgN *flgJ* *fliR* *flhA* *fliQ* *flgD* *flaF* *flgL* *flgK* *flgE* *fliK* *motC* *motB*

Bioinformatics

Čuklina et al., 2016

RT-PCR

Operon I

b   4   5   6   *flgG* *flgC*   7   8   a c

MS Ring | F | F | EA | B | LRi | ? | PRi | PRi | Dr | Pr | Pr | Pr | EA | CR | CR | ? | CR | M | *flgF1* *flgF2* *fliI*

fliF *lafA2* *lafA1* *fliP* *fliL* *flgH* *flgI* *flgA* *fliE* *flgB* *flhB* *fliG* *fliN* *fliM* *motA*

Op. I   Operon II   Operon III

Pr | Pr | EA

B

```
a - motA  CCTTCATGGCATAGGTGTAGAGGCGGTAGTCCTTCAGGAAGTCGTCGATCGTCTTCACGTTGCCGATATG/93/+1
b - fliF  CCAGATTTCAAGCAACACGCCGCAGCCGATCGCGCCGCGATGCGTCGGCCGTGCACCTGTTGCCGATCCT/112/+1
c – flgF1 CCGAGCAGCGCCGCCACCGTGATGAAAATCCCCACGAAACTGAGCAACGCGCCACTCCATCGCCGATCCC/90/+1
          *    :    *       *        *    **     *   ** * ******
```

FIG 2 Operons of the lateral-flagellar gene cluster, indicating the transcription directions according to Rhizobase (http://genome.annotation.jp/rhizobase/Bradyrhizobium). (A) The genes identified in the cluster are classified by function as regulators (R, gray), unknown (?, white), hook and hook-filament junction (H and HJ, violet), export apparatus (EA, green), motor (M, orange), MS ring (pink), flagellins (F, red), basal body (B, blue), L-ring and P-ring (LRi and PRi, turquoise), distal and proximal rods (Dr and Pr, light blue), and C-ring (CR, light pink). Below this scheme, the operon structure is indicated according to: bioinformatics prediction (upper light-pink line), Čuklina et al. (34) (middle light-pink line), and our own results from RT-PCR (bottom light-pink line). Above the scheme, the positions of the deduced *lafR*-dependent promoters are shown as black arrows, and the positions of the intergenic amplicons predicted according to the RT-PCR strategy outlined in Fig. S4 in the supplemental material are shown as black segments numbered from 1 to 8. For the sake of simplicity, the L subscripts in the figure have been omitted from the name of each locus. (B) Sequence alignment of the conserved motifs found upstream from the transcription start sites (designated as +1) of the genes *motA* (row a), *fliF*$_L$ (row b), and *flgF*$_L$*1* (row c), the latter being located at the 5′ ends of operons I, II, and III, respectively (see panel A). The consensus sequence that may be deduced is indicated at the bottom of the panel.

use of different bioinformatic tools (e.g., MicrobesOnline Database, ProOpDb, and DOOR[2]), we predicted the operon structure of the gene cluster that is schematized in Fig. 2A and found a new open reading frame between *fliR*$_L$ (bll6849) and *flgJ*$_L$ (bll6850), whose sequence we named bll6849.5. According to this analysis, the lateral-flagellar gene cluster might be divided into at least five putative operons and three monocistronic transcriptional units: *lafR*, *lafA1*, and *lafA2*. All transcriptional units are conserved in *E. meliloti* and *B. melitensis*, but the synteny contains some differences (see Fig. S3 in the supplemental material). In a recent study, a genome-wide transcription start site map for *B. diazoefficiens* USDA 110 grown in peptone/salts/yeast extract/arabinose medium was established (34), indicating different operon structures for the lateral-flagellar region from those predicted by the bioinformatic analysis (Fig. 2A). To resolve this contradiction, we designed primers to amplify, by reverse transcription-PCR (RT-PCR), eight intergenic regions that should differ in the resulting transcripts according to whether the distribution of polycistronic mRNAs from this genomic cluster under our conditions is as predicted by bioinformatics or as reported in the experimental tran-
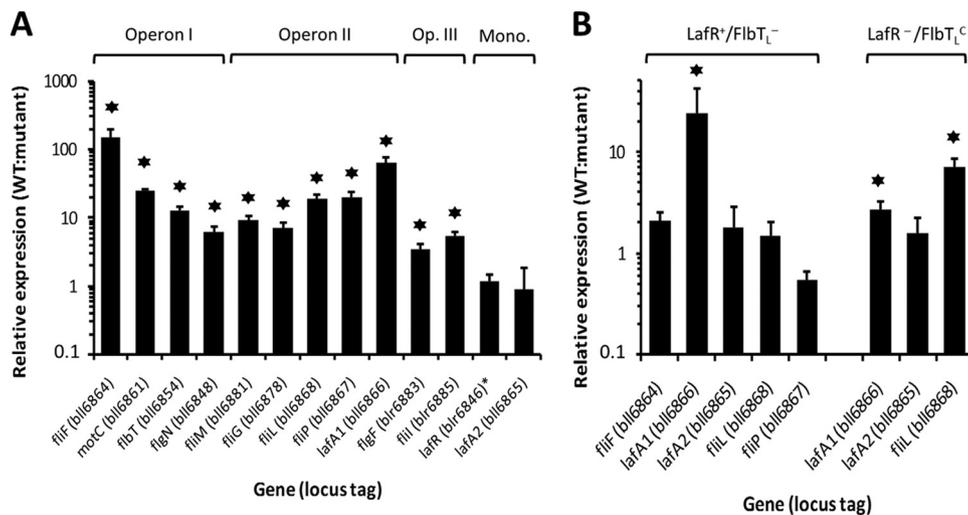
FIG 3 Effects of mutations in *lafR* and *flbT*$_L$ on the mRNA accumulation of selected lateral-flagellar genes. (A) Transcription expression level in the wild-type strain relative to that of the *lafR*::Km mutant plus the standard deviations (SD), as determined by qRT-PCR from at least three independent biological replicas for the indicated genes (locus tags), the latter being representative of the different transcriptional units. Mono., monocistronic transcripts. The relative expression of *lafR* was evaluated with the primers indicated in Fig. S2B in the supplemental material, which amplify the 5′ end of *lafR* both in the wild-type and in the *lafR*::Km mutant. Stars, statistically significant differences ($P < 0.05$) from a threshold interval of 0.5 to 2.0 according to the Student *t* test. (B) Transcription expression level in the wild-type strain relative to that of the Δ*flbT*$_L$ strain (LafR$^+$/FlbT$_L^-$, left) or that of *lafR*::Km carrying the plasmid pFAJ::*flbT*$_L$ (LafR$^-$/FlbT$_L^C$, right) $\pm$ the SD, as determined by qRT-PCR from at least three independent biological replicas for the indicated genes, the latter having been selected to indicate the differential influence of *flbT*$_L$ on *lafA1* expression. Stars, statistically significant differences ($P < 0.05$) from a threshold interval of 0.5 to 2.0 according to the Student *t* test. For the sake of simplicity, the L subscripts in the figure have been omitted from the name of each locus.

scription start site mapping (34). The regions chosen were as follows: region 1 from 3′ *flgJ*$_L$ (bll6849) to 5′ *fliR*$_L$ (bll6850; further encompassing the intergenic regions upstream and downstream from bll6849.5), region 2 from 3′ *flgE*$_L$ (bll6858) to 5′ bll6859, region 3 from 3′ *fliK*$_L$ (bll6860) to 5′ *motC* (bll6861), region 4 from 3′ *fliF*$_L$ (bll6864) to 5′ *lafA2* (bll6865), region 5 from 3′ *lafA2* (bll6865) to 5′ *lafA1*(bll6866), region 6 from 3′ *lafA1* (bll6866) to 5′ *fliP*$_L$ (bll6867), region 7 from 3′ *flgB*$_L$ (bll6876) to 5′ *flhB*$_L$ (bll6877), and region 8 from 3′ *fliN*$_L$ (bll6879) to 5′ bll6880 (Fig. 2A). By this approach, we would be able to detect amplification only where the mRNA is polycistronic for the adjacent genes probed (35). We observed that no amplification occurred only between 3′ *fliF*$_L$ and 5′ *lafA2*, and between 3′ *lafA2* and 5′ *lafA1* (see Fig. S4 in the supplemental material), suggesting the existence of two operons encompassing bll6847-*fliF*$_L$ (operon I) and *lafA1-motA* (operon II), with *lafA2* remaining as a monocistronic transcriptional unit situated between those two operons. In addition, *lafR* and *flgF1*$_L$-*fliI*$_L$ (operon III) can be considered different transcriptional units since they are contained in the opposite strand (Fig. 2A).

LafR activation of three of the four transcriptional units. We analyzed the requirements for LafR with respect to the transcriptional profile of the lateral flagellar regulon by quantitative reverse transcription-PCR (qRT-PCR) with whole RNA from the wild type and the *lafR*::Km mutant. We chose as representative genes of each transcriptional unit—*fliF*$_L$, *motC*, *flbT*$_L$, and *flgN*$_L$ for operon I; *fliM*$_L$, *fliG*$_L$, *fliL*$_L$, *fliP*$_L$, and *lafA1* for operon II; and *flgF1*$_L$ and *fliI*$_L$ for operon III—along with the monocistronic transcriptional units *lafR* and *lafA2* (Fig. 2A) for amplification. Figure 3A summarizes the results of the qRT-PCR assays. According to the relative expression levels obtained with the *lafR*::Km mutant in comparison to the wild type, we observed that *lafR* was not autoregulated but that, with respect to operons I to III, *lafR* was a positive regulator, a finding in agreement with the previous observation that the *lafR*::Km mutant was unable to produce lateral flagellins (Fig. 1). In contrast, mutation of *lafR* did not produce substantial changes in the abundance of the *lafA2* transcript.
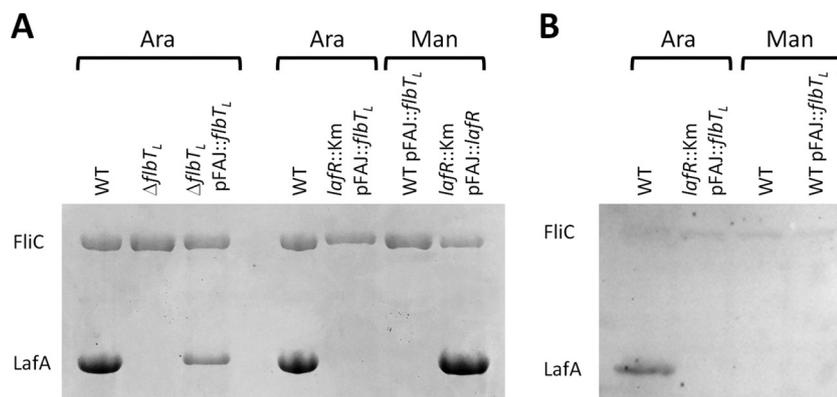
FIG 4 Control of flagellin expression by *flbT$_L$* in bacteria grown in liquid HMY medium with arabinose (Ara) or mannitol (Man) as carbon source. (A) SDS-PAGE of the *B. diazoefficiens* extracellular subpolar (FliC) and lateral (LafA) flagellins in the wild-type, the Δ*flbT$_L$* strain, the Δ*flbT$_L$* strain complemented with the plasmid pFAJ:: *flbT$_L$* that carries a wild-type copy of *flbT$_L$* under the direction of the *nptII* promoter, or the *lafR*::Km strain complemented with the plasmid pFAJ::*flbT$_L$* or pFAJ::*lafR*. (B) Western blots of the cellular *B. diazoefficiens* proteins FliC and LafA, as visualized by an anti-*lafA* polyclonal antiserum, from the wild-type strain either alone or complemented with the plasmid pFAJ::*flbT$_L$* or from the *lafR*::Km strain complemented with the plasmid pFAJ::*flbT$_L$*. The polyclonal anti-*lafA* serum exhibited some cross-reaction against FliC, whose activity in this experiment served as an internal standard.

To search for possible common motifs in the 5′ untranslated regions (5′ UTRs) of the three operons, we performed sequence comparisons with the MEME Suite (36). A *de novo* search for these sequences located a possible common motif shared by the LafR-induced operons (Fig. 2B). The motif is located approximately at the same distance from the transcription start site base pair (+1) of each operon. Of relevance here is that a search with the MAST algorithm at the MEME server did not locate this motif either upstream from the *E. meliloti rem* sequence—a finding in agreement with the lack of cross-complementation between *lafR* and *rem*—or upstream from any other *B. diazoefficiens* gene, suggesting that this motif might be shared by the *lafR*-dependent promoters.

The lack of changes in *lafA2* transcript accumulation between the wild type and the *lafR*::Km mutant indicates that another regulation is likely to be responsible for the inhibition of LafA2 polypeptide production in this mutant. We suspected that this role might be fulfilled by FlbT, a protein known as a translational regulator of flagellin synthesis in other bacteria (37, 38).

FlbT$_L$ as a positive regulator of flagellin synthesis. To investigate whether or not FlbT$_L$ regulates flagellin synthesis in *B. diazoefficiens* as in other bacteria, we constructed a *flbT$_L$* deletion mutant by eliminating 195 bp from the middle of the coding region (between bases 7549514 and 7549709) without any alteration in the reading frame (see Fig. S5 in the supplemental material). This mutant (Δ*flbT$_L$*) would thus be expected to produce an internally deleted gene product without any polar effects on genes downstream in the operon. We observed that the Δ*flbT$_L$* (LafR$^+$/FlbT$_L$$^-$) mutant was unable to produce LafA1 and LafA2 with arabinose as the carbon source and that this phenotype was reversed when the Δ*flbT$_L$* mutant was complemented in *trans* with a wild-type copy of *flbT$_L$* carried in the replicative plasmid pFAJ::*flbT$_L$* (Fig. 4A). Likewise, the Δ*flbT$_L$* mutant swimming motility in soft agar was compromised, similar to the analogous defect in Δ*lafA* and *lafR*::Km mutants, and this phenotype was partially complemented in *trans* (Fig. 1C). These results indicated that, as in *B. melitensis* (38), FlbT$_L$ is required for lateral flagellin synthesis.

Next, we extended the analysis of the transcriptional profile of the lateral-flagellar operons by incorporating an LafR$^-$/FlbT$_L$^{C} strain (*lafR*::Km mutant complemented with *flbT$_L$* in *trans* under the control of a constitutive promoter). Using the same approach as before (Fig. 3A), we compared the relative expression of *motC* and *fliF$_L$* (operon I), *fliM$_L$*, *fliL$_L$*, and *lafA1*(operon II), and *lafA2* in the wild type to both LafR$^+$/FlbT$_L$$^-$ and the
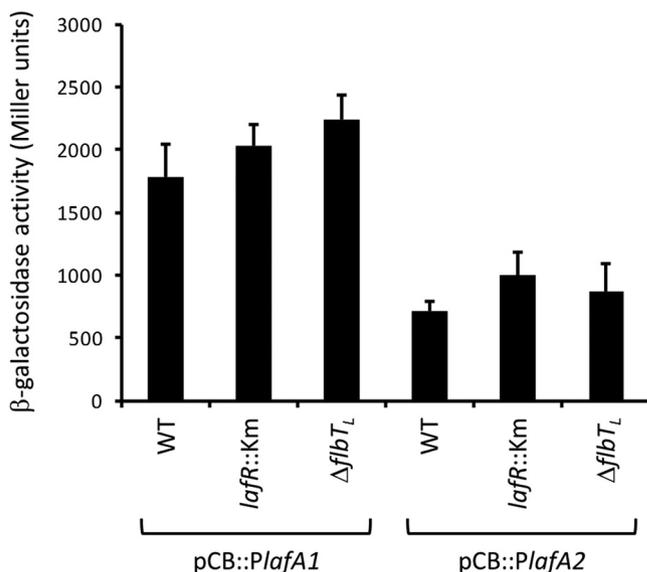
FIG 5 β-Galactosidase activities of pCB::P*lafA1* and pCB::P*lafA2 lacZ* fusions within three genetic backgrounds. In the figure, the β-galactosidase activity in Miller units is plotted on the ordinate for each of the genetic backgrounds denoted on the abscissa. The two clonal fusions are indicated in brackets below the figure. Each mean value is from two independent clones measured in duplicate. Error bars indicate the SD.

LafR$^-$/FlbT$_L$^{C} genetic backgrounds. We observed that the deletion of *flbT$_L$* had no effect on the expression of any of the genes tested, except for *lafA1*: in this gene, however, transcript accumulation was inhibited when *flbT$_L$* bore a mutation similar to that of *lafR* (Fig. 3B). Because *flbT$_L$* was itself induced by *lafR*, the observed effect of the *lafR* mutation on *lafA1* expression could be indirect as a result of a downregulation of *flbT$_L$* within the *lafR*::Km genetic background. Therefore, we evaluated the expression of *lafA1* in the LafR$^-$/FlbT$_L$^{C} genetic background and observed that the transcript accumulation of *lafA1* was partially restored, although the relative expression of *lafA1* in the wild type with respect to that of the mutant was still significant, indicating that *flbT$_L$* had a partial influence on the control of *lafA1* transcript accumulation. Conversely, the adjacent gene *fliL$_L$* within the same operon responded only to *lafR* since that locus was downregulated within the LafR$^-$/FlbT$_L$^{C} genetic background (similar to the result with the *lafR*::Km mutant) but was not affected in the LafR$^+$/FlbT$_L$$^-$ background (Fig. 3B).

Although a transcription start site of *lafA1* could not be detected by RNA sequencing analysis (34), the pattern of differential regulation on the part of *lafA1* with respect to the rest of operon II prompted us to investigate whether an internal promoter activity might be found within operon II upstream from *lafA1*. To this end, we cloned the DNA segments between the 3′ end of *fliP$_L$* and the ATG of *lafA1* (P*lafA1*) and between the 3′ end of *lafA1* and the ATG of *lafA2* (P*lafA2*) in the replicative plasmid pCB303 upstream from the promoterless *lacZ* site and measured the resultant β-galactosidase activity of the fusions. We observed more than twice the activity in the pCB::P*lafA1* plasmid carrying the P*lafA1*::*lacZ* fusion than in the pCB::P*lafA2* plasmid carrying the P*lafA2*::*lacZ* fusion, without differences among the wild-type, *lafR*::Km, and Δ*flbT$_L$* genetic backgrounds (Fig. 5), thus indicating the existence of an active promoter upstream from *lafA1*, whose locus—as with *lafA2*—would not be under transcriptional control of LafR or FlbT$_L$. To further investigate the difference in the responses of *lafA1* and *lafA2* to FlbT$_L$, we compared the nucleotide sequences and RNA predicted structures of the 5′ UTRs of these transcripts. To this end, we used the sequence within the *lafA2* 5′ UTR beginning at the experimentally identified transcription start site located 118 nucleotides upstream from the ATG initiation codon (34) and extending through the first 17 codons of the coding sequence (39) in comparison to a putative 5′ UTR of *lafA1* starting also 118 nucleotides upstream from the ATG and continuing through the

first 17 codons of the coding sequence. Despite the high conservation among these sequences, we observed a gap near a sequence complementary to the ribosome binding site (RBS) in *lafA2* (see Fig. S6A in the supplemental material). In four of seven predicted stable secondary structures of the *lafA1* 5′ UTR region, a small loop arose at the RBS complementary sequence, whose conformation might loosen RBS occlusion but would leave the ATG initiation codon in a double-helix stretch (see Fig. S6B in the supplemental material). In contrast, the other three structures, as well as the two predicted stable secondary structures of the *lafA2* 5′ UTR, had the RBS site in a double-helix stretch, but the ATG start codon was predicted in a single-strand region (see Fig. S6B and C in the supplemental material). Taken together, these results are consistent with the postulated presence of a constitutive internal active promoter in operon II for *lafA1* transcription. The most plausible assumption to explain the above results may be that *lafA1* mRNA stability might be controlled by $FlbT_L$ differently from that of *lafA2* (Fig. 2A).

Despite *lafA1* and *lafA2* transcript production, lateral flagellins were observed in neither *B. diazoefficiens* USDA 110 carrying pFAJ::*flbT_L* cultured with mannitol nor the *lafR*::Km mutant carrying pFAJ::*flbT_L* cultured with arabinose (Fig. 4A). We reasoned that these observations might be due to the lack of a filament export apparatus under conditions where LafR is not produced, thus leading to an accumulation of LafA1 and LafA2 inside the cell. To test for this possibility, we obtained total cellular proteins and performed a Western blot with an LafA-specific polyclonal antibody (22). As expected, the wild-type *B. diazoefficiens* cultured with mannitol did not accumulate LafA intra-cellularly, whereas the same strain cultured with arabinose contained a clearly visible band of binding by the anti-LafA antibody in the Western blot at the expected molecular mass. In contrast, complementation with *flbT_L* in *trans* failed to restore LafA accumulation in either the wild-type cells grown with mannitol or the *lafR*::Km mutant grown with arabinose, where *lafR* was not expressed (Fig. 4B).

DISCUSSION

The lateral-flagellar genes of *B. diazoefficiens* lie in a single cluster encompassing 34,823 bp, organized in two monocistronic transcriptional units and three operons, with one of those three possibly having an independent internal promoter. In addition, no chemotaxis genes are present in this cluster. The expression of the three operons required the protein product of *lafR*; this gene constitutes one of the monocistronic transcriptional units identified. The regulation of LafR, together with the protein's sequence homology to known class IB master regulators, suggests that LafR is the class IB master regulator of lateral flagellum synthesis in *B. diazoefficiens*. In alphaproteo-bacteria there are different types of master regulators, including two-component systems such as the *ctrA-cckA* of *Rhodobacter capsulatus* (40) or OmpR-like transcriptional activators such as the *rem* of *E. meliloti* (28) or the *ftcR* of *B. melitensis* (32). These latter activators, in turn, are controlled by the respective LuxR-type systems, *visNR* and *vjbR* (32, 41, 42), which respond to cell cycle cues or environmental stimuli, indicating the need to activate or inactivate flagellar synthesis. In the particular example of *B. diazoefficiens*, the respiration rate might be just such a signal linked to the transcription of the lateral-flagellar regulon. Previous reports indicated that situations diminishing the respiration rate, such as microaerobiosis, the bacteroid state (23), or iron deficiency (24), downregulate the lateral-flagellar regulon transcription, whereas situations known to increase the oxygen consumption, such as permanent exposure to moderate oxidative stress (25) or the use of arabinose as the sole carbon source (43; C. Cogo, J. Pérez-Giménez, C. B. Rajeswari, M. F. Luna, and A. R. Lodeiro, unpublished data), promote that transcription. Moreover, these changes in transcription were not observed in the subpolar-flagellar regulon, indicating that these stimuli act specifically on the lateral flagella. Although we could not find *visNR* or *vjbR* homologs in *B. diazoefficiens*, the RegSR two-component system—which regulates the responses to microoxia—was reported to modify the expression specifically of *lafR* and the lateral-flagellar regulon after a switch from oxic to microoxic (O_2 concentration $< 0.5\%$)

conditions (44). In agreement with these results, a TetR family transcriptional regulator was also found to repress the lateral-flagellar genes in a coordinated manner, along with genes encoding high-affinity cytochromes and oxidative-stress detoxification products, without affecting the subpolar-flagellar genes (45). Therefore, several stimuli related to the energy status of the cell are able to trigger lateral-flagellar expression in *B. diazoefficiens* without affecting subpolar-flagellar expression. Such stimuli seem transmitted to the class IB regulator *lafR* by different class IA regulators from those of *E. meliloti* or *B. melitensis*. In turn, *lafR* itself could be part of a two-component system, but two observations argue against this possibility. First, a putative histidine kinase could not be found for this system; second, the phosphorylatable Asp50 residue of LafR may be replaced by Ala, Gly, or Glu without alterations in the response of flagellin synthesis to the carbon source present in the culture medium, indicating that Asp50 is not phosphorylated in LafR.

The correlation between operon organization and flagellar substructures shown in Fig. S1 in the supplemental material indicates that all the genes induced by LafR are among the class II genes transcribed in the second step of the cascade, although the strict temporal order observed in other species (11) is not reflected by the distribution of the flagellar genes among the three operons. Most of the flagellar motor (4) is encoded in operon II, except the MS ring component $FliF_L$ and the stator protein MotB, both of whose loci are encoded in operon I. Moreover, the genes encoding the export apparatus (2, 3), whose component is also part of the basal body, are scattered among the three operons. The export of the hook and filament proteins from the cytoplasm to the extracellular space through the narrow space inside the rod may require (i) their recruitment at the export gate that is formed by $FlhA_L$, $FliQ_L$, and $FliR_L$ (operon I) and $FlhB_L$ and $FliP_L$ (operon II), (ii) ATP hydrolysis catalyzed by $FliI_L$ (operon III), (iii) the chaperon activities of $FlgN_L$ (operon I) and $FlgA_L$ (operon II), and (iv) the control switch in the export sequence between hook and filament effected by $FliK_L$ (operon I). The structure of the rod apparatus and the rings that act as bushings in the membranes and the peptidoglycan layer are mostly encoded in operon II, except for $flgF_L$, whose locus is in operon III. The gene $flgJ_L$ that encodes the β-*N*-acetylglucosaminidase required for the hydrolysis of the peptidoglycan layer in order to allow passage of the P-ring and the rod (46), however, is in operon I (see Fig. S1 in the supplemental material). Therefore, a functional export apparatus in this flagellar system requires the expression of genes from the three operons. Some genes are also missing—such as *fliD* encoding the filament cap and the *fliI*-associated *fliH* and *fliJ*—whose loci might be encoded in the hypothetical open reading frames that we could not yet identify. In addition, a complementation by proteins from the subpolar-flagellar system cannot be discarded, although this possibility seems unlikely in view of the substantial difference in structure and function between the two flagellar systems.

Moreover, operon I encodes $FlbT_L$, a regulator whose homologs in *C. crescentus* and *B. melitensis* regulate the expression of class III genes (37, 38). Despite that homology, however, FlbT plays opposite roles in those systems: whereas in *C. crescentus* FlbT is an inhibitor of the translation of flagellin transcripts, in *B. melitensis* that protein is required for translation. The target site of FlbT-dependent regulation—it is reported to lie within the 5′ UTR of the mRNA—regulates translation and mRNA stability, but the existence of an as-yet-unknown intermediate for the formation of the FlbT/5′ UTR/mRNA complex might explain these opposite actions (39). Moreover, some effect of FlbT on the activity of the flagellin gene promoter has also been detected (38, 47). In the example of the *B. diazoefficiens* lateral flagella, the role of $FlbT_L$ in *lafA1* and *lafA2* expression was even more intriguing. As in *B. melitensis*, $FlbT_L$ was required for lateral-flagellin production (Fig. 4), including LafA1 and LafA2 in the low-molecular-mass band (20); however, as a striking exception to the known flagellar systems, the flagellin gene *lafA1* lies at the 3′ end of operon II under transcriptional control of the class IB regulator LafR, instead of being a class III gene encoded in a monocistronic transcriptional unit. After an evaluation of the effects of LafR and $FlbT_L$ on $fliL_L$ and *lafA1* transcript accumulation (Fig. 3B), LafR activity proved to be only in part required for *lafA1* expression; this result
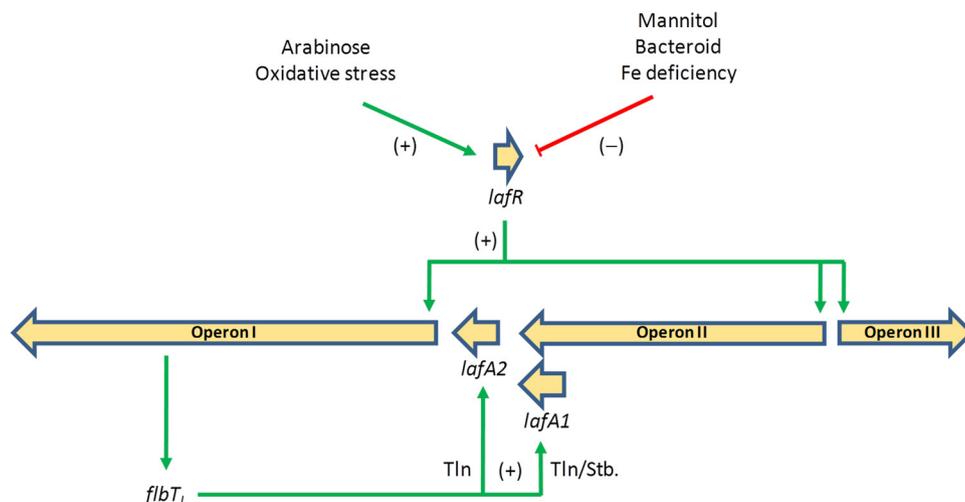
FIG 6 Scheme of the regulation of the lateral-flagellar genes that may be deduced from the present results. Cultivation with arabinose as the carbon source induces the expression of *lafR*, whereas cultivation with mannitol as the carbon source does not. LafR activates the transcription (Txn) of operons I, II, and III without any special hierarchical order among them, while the monocistronic *lafA2* is transcribed independently of LafR. Operon I contains *flbT$_L$*, whose locus, upon activation, acts as a translation (Tln) inducer of the monocistronic *lafA2* and appears to stabilize (Stb) the *lafA1* transcript from a promoter within operon II. In addition to the effects of arabinose and mannitol, evidence from the literature indicates that prolonged exposure to moderate oxidative stress also induces *lafR* and the lateral flagellar regulon (25), whereas situations of O$_2$ limitation as the bacteroid state (23) or iron limitation (24) repress them. We also observed that viscosity and tortuousity of the medium induce lateral flagella (20) and that microoxia was reported as inhibiting lateral flagella genes expression (23). Therefore, the signal to which the expression of lateral-flagellar genes responds might be related to the energy status of the cell, apart from the specific carbon source available.

is consistent with the existence of an internal promoter within operon II upstream of *lafA1*. The activity of this internal promoter would not be regulated by LafR or FlbT$_L$, but the differences in nucleotide sequence and predicted secondary structure between the 5′ UTRs of *lafA1* and *lafA2*, as well as the discrepancies in the responses of these genes to FlbT$_L$ with respect to transcript abundance, suggest that the *lafA1* transcript would be more unstable than the *lafA2* transcript in the absence of FlbT$_L$. Therefore, both the expression and the subsequent mRNA stability of *lafA1* seem to be under a mixture of class IB and class III regulation, whereas the *lafA2* monocistronic transcript would require neither LafR nor FlbT$_L$ for accumulation, and in this instance the role of FlbT$_L$ might be restricted to some form of translational control. Neither LafA1 nor LafA2 seemed to accumulate in the cytoplasm of cells expressing *flbT$_L$* from a multicopy plasmid when the export apparatus was not formed, indicating that an additional system coordinates LafA production and secretion. We identified *flaF$_L$* as being located immediately upstream from *flbT$_L$* in operon I. In *C. crescentus* and *B. melitensis* FlaF was described as a counterregulator of FlbT through an as-yet-unknown mechanism (38, 47). If FlaF$_L$ has a similar role in *B. diazoefficiens*, that protein might prevent FlbT-dependent translation of the *lafA2* and *lafA1* transcripts until the export apparatus becomes functional. Figure 6 presents the scheme of the regulatory circuit that may be deduced from our results.

The present results indicate that the hierarchies of regulation at the level of transcription are not as strict as in model systems but instead seem more similar to the regulation in *B. melitensis*, where the flagella are synthesized during a short period in the bacterial culture (38). This lack of a hierarchy might constitute an adaptation to the use of these flagella only when required by the environmental conditions. In the example of the lateral flagella of *B. diazoefficiens*, the environmental conditions seem to be related either to energy availability and demand—in particular the availability of oxygen (23) and the carbon source (the present study)—or to a requirement for higher torque by the flagella, such as upon an alteration in the viscosity and/or the porosity of the medium (20). Monitoring of these situations might be essential in order for this

bacterium to adapt its energy expenditures for motility to the soil's environmental dynamics.

MATERIALS AND METHODS

Bacterial strains and culture conditions. Table S1 in the supplemental material summarizes the bacterial strains and plasmids used in this work. *B. diazoefficiens* was grown in HM salts (48) plus 0.1% yeast extract (HMY) with 0.5% mannitol or 0.5% arabinose as the carbon source. Total biomass was estimated by measurement of the optical density at 500 nm (OD_{500}) and the number of viable bacteria by the number of CFU on yeast extract-mannitol (49) agar plates (YMA). For swimming-motility analysis, bacteria were inoculated with a sterile toothpick on semisolid AG medium (48) containing 0.3% (wt/vol) agar, and the motility halo was registered as described previously (21). For conjugation, a modified peptone salt-yeast extract medium (50) was used. *Escherichia coli* was grown in Luria-Bertani medium (51). Antibiotics were added to the media at the following concentrations (μg ml^{-1}): streptomycin, 400 (*B. diazoefficiens*) or 100 (*E. coli*); spectinomycin, 200 (*B. diazoefficiens*) or 100 (*E. coli*); kanamycin, 150 (*B. diazoefficiens*) or 25 (*E. coli*); ampicillin, 200; gentamicin (Gm), 100 (*B. diazoefficiens*) or 10 (*E. coli*); chloramphenicol (Cm), 20 (*B. diazoefficiens*); and tetracycline (Tc), 20 or 50 (*B. diazoefficiens* in liquid or solid cultures) or 10 (*E. coli*).

Bioinformatic methods. The multiple alignments were performed by means of CLUSTAL OMEGA (52) at the EMBL online server (53). The operon prediction was run in different online servers: the ProOpDB online server (54), the DOOR^2 online server (55), and the MicrobesOnline server tools (56). Analysis of these results in comparison to the transcription start site map of *B. diazoefficiens* (34) was carried out using the Integrated Genome Browser (57). All the oligonucleotides were designed with Primer BLAST (58). The RNA secondary structure prediction was carried out with Mfold 2.3 at 30°C with the other parameters as the default (59). To find the common motif in the upstream DNA sequences of operons I, II, and III, the MEME Suite was used (36). The scheme of the motif was built with the WebLogo server (60).

Genetic techniques and DNA manipulation. The cloning procedures— comprising DNA isolation, restriction digestion, ligation, and bacterial transformation—were performed as previously described (51). Bi- or triparental matings were performed with *E. coli* DH5α or S17-1, respectively, as previously described (61). Electroporation was performed with a GenePulser (Bio-Rad, Hercules, CA) at 1.5 V, 25 μF, and 200 Ω in a 0.1-cm-gap-width electroporation cuvette.

Oligonucleotide primers (see Table S1 in the supplemental material) were purchased from Life Technologies (Buenos Aires, Argentina). DNA amplification was performed by using PCR in a Bioer Life Express thermocycler (Hangzhou, China) with *Taq* DNA polymerase (Life Technologies, Buenos Aires, Argentina) for routine PCR or with KAPA HiFi hot start (HS) DNA polymerase (Kapabiosystems, Woburn, MA) for amplification of targets longer than 1,000 bp. The DNA sequencing was performed at Macrogen Corp. (Seoul, South Korea).

To construct the *B. diazoefficiens lafR*::Km mutant, specific primers for blr6846 were designed. The fragment between bp 7542881 and 7543632 was amplified from the *B. diazoefficiens* USDA 110 genomic DNA and cloned into the plasmid pG18mob2 (62) by means of an internal EcoRI site (at bp 7542999) and a HindIII site generated from the LafR_Rv primer to generate the plasmid pG::*lafR*. Next, the Km cassette from the plasmid pUC4K (63) was cloned into an internal BamHI site (at bp 7543291) of the *lafR* fragment to give plasmid pG::*lafR*::Km. The gene insertion of the Km cassette was performed by introducing the pG::*lafR*::Km into *B. diazoefficiens* wild-type strain USDA 110 by biparental mating, with recombinant selection by growth on Km/Cm YMA, with subsequent screening for Km resistance and Gm sensitivity in order to select for the double-crossover mutant. The resulting strain was designated *lafR*::Km; this strain carries the Km cassette insertion at the position 7543291 of the genomic DNA, thus disrupting the connection between the receiver and the helix-turn-helix domains of *lafR* (see Fig. S2B in the supplemental material).

The point mutations in the residue susceptible to phosphorylation (Asp50; see Fig. S2A in the supplemental material) were performed as described previously (51). In brief, PCR primers were designed complementary to the region spanning the mutation site of plasmid pG::*lafR*—that plasmid DNA being the template for the reaction—but with single complementary base changes for one residue in both strands of the site in order to generate the desired point mutation. The PCR under the direction of those primers then amplified with *Pfu* DNA polymerase (Thermo Fisher Scientific, Waltham, MA) the entire plasmid, including the mutation introduced in the primers, to give the double-stranded DNA for the new mutant plasmid. The PCR mix was then treated with DpnI, and the template was degraded. The reaction mix was desalted and transformed into *E. coli* DH5α. Because the position of the point mutation coincides with a SalI restriction site in the wild-type sequence, we screened the clones by looking for resistance to digestion with this endonuclease. The positive clones were then corroborated by DNA sequencing. The fragments with the point mutation were subcloned in the plasmid vector pK18*mobsacB* (64) to give the derivatives pK*sacB*::*lafR*D50A, pK*sacB*::*lafR*D50G, and pK*sacB*::*lafR*D50E. Each plasmid was transferred by mating to the wild-type strain, and simple crossovers were selected by Km resistance. Resolution of the plasmid was forced by plating the Km-resistant colonies in YMA supplemented with 10% (wt/vol) sucrose. The resulting clones were corroborated by PCR amplification and SalI digestion of the fragment.

To construct the *B. diazoefficiens* Δ*flbT$_L$* mutant, the crossover PCR method described by Link et al. (65) was applied to generate an in-frame deletion of the coding sequence of bll6854 (*flbT$_L$*). To this end, specific primers (FlbTUP_w and FlbTUP_Rv for PCR 1 and FlbTDW_Fw and FlbTDW_Rv for PCR 2) were designed for the amplification of upstream (118-bp) and downstream (99-bp) fragments of *flbT$_L$* (PCR 1 and PCR 2 according to the methods in the references cited). Next, a PCR 3 reaction was run with primers

FlbTUP_Fw and FlbTDW_Rv with an equal mixture of PCR 1 and PCR 2 products as the template. The product of this PCR contains the 5′ and 3′ portions of $flbT_L$ interrupted by a short synthetic sequence (21 bp) that replaces an internal 195-bp fragment of the 411-bp coding sequence of $flbT_L$ without affecting the reading frame (see Fig. S5 in the supplemental material). This construct was cloned into the pK18*mobsacB* vector to yield plasmid pK*sacB*::$flbT_L$. This plasmid was transferred to the wild-type strain by biparental mating, and a resulting single crossover was selected by Km resistance. These simple recombinants were selected for further double crossovers by plating the bacteria in YMA supplemented with 10% (wt/vol) sucrose; thereafter, the resulting clones were subjected to PCR to distinguish the wild-type resolution of the plasmid from the mutant genotype. The correct in-frame deletion was verified by DNA sequencing.

Complementation experiments were performed by integrating the complete sequences of *lafR* or $flbT_L$ (amplified with the primer pair LafRextFw/LafRextRv or FlbTextFw/FlbTextRv, respectively) into a replicative vector. Stated in brief, the 1,009-bp *lafR* and the 592-bp $flbT_L$ target sequences were amplified from *B. diazoefficiens* USDA 110 chromosomal DNA and then cloned into the XbaI/KpnI sites of plasmid pFAJ1708 to create pFAJ::*lafR* and pFAJ::$flbT_L$, respectively. The recombinant plasmids were cloned with the *lafR* or $flbT_L$ genes under the direction of the strong, constitutive *nptII* promoter (66). These constructions were all confirmed by sequencing. Finally, each plasmid harboring the complete *lafR* or $flbT_L$ gene was transferred into the desired *B. diazoefficiens* strain by biparental mating, selected by Tc resistance, and confirmed by PCR amplification and DNA sequencing.

To construct the *lacZ* fusions, the *lafA1* and *lafA2* promoter regions were amplified with the primer pairs promA1_Fw/promA1_Rv and promA2_Fw/promA2_Rv, respectively (see Table S1 in the supplemental material). The amplicons were digested with XbaI/PstI and then cloned into the same restriction sites of the promoterless plasmid vector pCB303 carrying the complete sequence of the β-galactosidase gene (67). These constructions were named pCB::P*lafA1* and pCB::P*lafA2*, respectively. Each plasmid was transferred into the *B. diazoefficiens* USDA 110 strain by biparental mating, selected by Tc resistance, and confirmed by PCR amplification. The β-galactosidase activity was measured as described previously (51).

RNA extraction and RT-PCR. Portions (13 ml) of *B. diazoefficiens* USDA 110 cells were harvested from liquid cultures, washed twice with 1 M NaCl, and disrupted with lysozyme in Tris-EDTA buffer (pH 8.0, 30 min, 37°C). Total RNA was extracted through the use of TRIzol (Life Technologies, Buenos Aires, Argentina), according to the manufacturer's instructions, and the quality and quantity of the extract determined with a NanoDrop spectrophotometer (NanoDrop Technologies, Wilmington, DE). Aliquots (0.125 μg) were treated with DNase I (30 min, 37°C), and the cDNA synthesized with Moloney murine leukemia virus reverse transcriptase (Life Technologies, Buenos Aires, Argentina) under the direction of random hexamer primers according to the manufacturer's instructions. To check the quality of the cDNA preparation, PCRs were performed with the primer pairs *phaR*_Fw/*phaR*_Rv and *relA*_Fw/*relA*_Rv (see Table S1 in the supplemental material) as described previously (61). The absence of contaminating DNA was demonstrated by the lack of PCR amplification in an RNA sample that was not subjected to reverse transcription. Primers for the housekeeping gene s*igA* were used as a positive control (68).

To determine the operon structure, three RT-PCRs were performed with the appropriate cDNAs for each fragment (see Fig. S4): two of the reactions amplified fragments of the coding sequence of each contiguous gene (positive control), while the third amplified a fragment encompassing the intergenic region between the target genes (35).

Quantitative real-time RT-PCR. Amplification of the cDNAs obtained as described above was performed with the primers indicated in the Table S1 in the supplemental material for each gene in a Line-Gene instrument (Bioer, Hangzhou, China) and analyzed with Line-Gene K fluorescence quantitative detection system (v4.0.00 software). Ready-to-use iQ SYBR green Supermix (Bio-Rad, Hercules, CA) was used for all the reactions, according to the manufacturers' instructions. Normalized expression values were calculated based on the absolute quantities of the gene of interest relative to the value for *sigA* (68).

Flagellin separation and analysis. The preparation of flagellins was carried out as described previously (30). Stated in brief, rhizobia grown in liquid medium to an OD_{500} of 1.0 were vortexed for 5 min and centrifuged at 10,000 × *g* for 30 min at 4°C. The supernatant was collected and incubated with 1.3% (vol/vol) polyethylene glycol 6000 and 166 mM NaCl for 2 h at 4°C. This suspension was centrifuged at 11,000 × *g* for 40 min at 4°C, and the pellet resuspended in phosphate-buffered saline. For analysis, the samples were boiled in Laemmli loading buffer for 10 min and then separated by SDS-PAGE (69). Polypeptide bands were revealed with Coomassie brilliant blue R250.

Total proteins were prepared after lysis by boiling. The cell pellet was washed with 1 M NaCl solution, resuspended in Laemmli loading buffer, and heated for 10 min at 100°C. The samples were then centrifuged at 14,000 × *g* for 10 min and analyzed by SDS-PAGE. After electrophoresis, the gels were stained with Coomassie brilliant blue R250. Western blots were prepared with specific anti-LafA polyclonal antibodies on the total proteins extracted from the cell pellets, as previously described (22, 70).

SUPPLEMENTAL MATERIAL

Supplemental material for this article may be found at https://doi.org/10.1128/JB .00253-17.

SUPPLEMENTAL FILE 1, PDF file, 1.0 MB.

ACKNOWLEDGMENTS

REFERENCES

1. Yuan J, Branch RW, Hosu BG, Berg HC. 2012. Adaptation at the output of the chemotaxis signaling pathway. Nature 484:233–236. https://doi.org/10.1038/nature10964.

2. Evans LD, Hughes C, Fraser GM. 2014. Building a flagellum outside the bacterial cell. Trends Microbiol 22:566–572. https://doi.org/10.1016/j.tim.2014.05.009.

3. Minamino T. 2014. Protein export through the bacterial flagellar type III export pathway. Biochim Biophys Acta 1843:1642–1648. https://doi.org/10.1016/j.bbamcr.2013.09.005.

4. Minamino T, Imada K. 2015. The bacterial flagellar motor and its structural diversity. Trends Microbiol 23:267–274. https://doi.org/10.1016/j.tim.2014.12.011.

5. Takekawa N, Nishiyama M, Kaneseki T, Kanai T, Atomi H, Kojima S, Homma M. 2015. Sodium-driven energy conversion for flagellar rotation of the earliest divergent hyperthermophilic bacterium. Sci Rep 5:12711. https://doi.org/10.1038/srep12711.

6. Berg HC. 2016. The flagellar motor adapts, optimizing bacterial behavior. Prot Sci https://doi.org/10.1002/pro.305.

7. Fujii T, Kato T, Namba K. 2009. Specific arrangement of alpha-helical coiled coils in the core domain of the bacterial flagellar hook for the universal joint function. Structure 17:1485–1493. https://doi.org/10.1016/j.str.2009.08.017.

8. Calladine CR, Luisi BF, Pratap JV. 2013. A "mechanistic" explanation of the multiple helical forms adopted by bacterial flagellar filaments. J Mol Biol 425:914–928. https://doi.org/10.1016/j.jmb.2012.12.007.

9. Magariyama Y, Ichiba M, Nakata K, Baba K, Ohtani T, Kudo S, Goto T. 2005. Difference in bacterial motion between forward and backward swimming caused by the wall effect. Biophys J 88:3648–3658. https://doi.org/10.1529/biophysj.104.054049.

10. McCarter LL. 2006. Regulation of flagella. Curr Opin Microbiol 9:180–186. https://doi.org/10.1016/j.mib.2006.02.001.

11. Altegoer F, Bange G. 2015. Undiscovered regions on the molecular landscape of flagellar assembly. Curr Opin Microbiol 28:98–105. https://doi.org/10.1016/j.mib.2015.08.011.

12. Aldridge P, Hughes KT. 2002. Regulation of flagellar assembly. Curr Opin Microbiol 5:160–165. https://doi.org/10.1016/S1369-5274(02)00302-8.

13. Brown J, Faulds-Pain A, Aldridge P. 2009. The coordination of flagellar gene expression and the flagellar assembly pathway, p 99–120. In Jarrel KF (ed), Pili and flagella: current research and future trends. Caister Academic Press, Trowbridge, Wiltshire, United Kingdom.

14. Smith TG, Hoover TR. 2009. Deciphering bacterial flagellar gene regulatory networks in the genomic era. Adv Appl Microbiol 67:257–295. https://doi.org/10.1016/S0065-2164(08)01008-3.

15. Gotz R, Schmitt R. 1987. *Rhizobium meliloti* swims by unidirectional, intermittent rotation of right-handed flagellar helices. J Bacteriol 169:3146–3150. https://doi.org/10.1128/jb.169.7.3146-3150.1987.

16. Scharf B. 2002. Real-time imaging of fluorescent flagellar filaments of *Rhizobium lupini* H13-3: flagellar rotation and pH-induced polymorphic transitions. J Bacteriol 184:5979–5986. https://doi.org/10.1128/JB.184.21.5979-5986.2002.

17. Wei Y, Wang X, Liu J, Nemenman I, Singh AH, Weiss H, Levin BR. 2011. The population dynamics of bacteria in physically structured habitats and the adaptive virtue of random motility. Proc Natl Acad Sci U S A 108:4047–4052. https://doi.org/10.1073/pnas.1013499108.

18. Sourjik V, Wingreen NS. 2012. Responding to chemical gradients: bacterial chemotaxis. Curr Opin Cell Biol 24:262–268. https://doi.org/10.1016/j.ceb.2011.11.008.

19. Liu R, Ochman H. 2007. Origins of flagellar gene operons and secondary flagellar systems. J Bacteriol 189:7098–7104. https://doi.org/10.1128/JB.00643-07.

20. Quelas JI, Althabegoiti MJ, Jimenez-Sanchez C, Melgarejo AA, Marconi VI, Mongiardini EJ, Trejo SA, Mengucci F, Ortega-Calvo JJ, Lodeiro AR. 2016. Swimming performance of *Bradyrhizobium diazoefficiens* is an emergent property of its two flagellar systems. Sci Rep 6:23841. https://doi.org/10.1038/srep23841.

21. Althabegoiti MJ, López-García SL, Piccinetti C, Mongiardini EJ, Pérez-Giménez J, Quelas JI, Perticari A, Lodeiro AR. 2008. Strain selection for improvement of *Bradyrhizobium japonicum* competitiveness for nodulation of soybean. FEMS Microbiol Lett 282:115–123. https://doi.org/10.1111/j.1574-6968.2008.01114.x.

22. Covelli JM, Althabegoiti MJ, López MF, Lodeiro AR. 2013. Swarming motility in *Bradyrhizobium japonicum*. Res Microbiol 164:136–144. https://doi.org/10.1016/j.resmic.2012.10.014.

23. Pessi G, Ahrens CH, Rehrauer H, Lindemann A, Hauser F, Fischer HM, Hennecke H. 2007. Genome-wide transcript analysis of *Bradyrhizobium japonicum* bacteroids in soybean root nodules. Mol Plant Microbe Interact 20:1353–1363. https://doi.org/10.1094/MPMI-20-11-1353.

24. Yang J, Sangwan I, Lindemann A, Hauser F, Hennecke H, Fischer HM, O'Brian MR. 2006. *Bradyrhizobium japonicum* senses iron through the status of haem to regulate iron homeostasis and metabolism. Mol Microbiol 60:427–437. https://doi.org/10.1111/j.1365-2958.2006.05101.x.

25. Donati AJ, Jeon JM, Sangurdekar D, So JS, Chang WS. 2011. Genome-wide transcriptional and physiological responses of *Bradyrhizobium japonicum* to paraquat-mediated oxidative stress. Appl Environ Microbiol 77:3633–3643. https://doi.org/10.1128/AEM.00047-11.

26. Wei X, Bauer WD. 1998. Starvation-induced changes in motility, chemotaxis, and flagellation of *Rhizobium meliloti*. Appl Environ Microbiol 64:1708–1714.

27. Fretin D, Fauconnier A, Kohler S, Halling S, Leonard S, Nijskens C, Ferooz J, Lestrate P, Delrue RM, Danese I, Vandenhaute J, Tibor A, DeBolle X, Letesson JJ. 2005. The sheathed flagellum of *Brucella melitensis* is involved in persistence in a murine model of infection. Cell Microbiol 7:687–698. https://doi.org/10.1111/j.1462-5822.2005.00502.x.

28. Rotter C, Muhlbacher S, Salamon D, Schmitt R, Scharf B. 2006. Rem, a new transcriptional activator of motility and chemotaxis in *Sinorhizobium meliloti*. J Bacteriol 188:6932–6942. https://doi.org/10.1128/JB.01902-05.

29. Hoang HH, Gurich N, González JE. 2008. Regulation of motility by the ExpR/Sin quorum-sensing system in *Sinorhizobium meliloti*. J Bacteriol 190:861–871. https://doi.org/10.1128/JB.01310-07.

30. Althabegoiti MJ, Covelli JM, Pérez-Giménez J, Quelas JI, Mongiardini EJ, López MF, López-García SL, Lodeiro AR. 2011. Analysis of the role of the two flagella of Bradyrhizobium japonicum in competition for nodulation of soybean. FEMS Microbiol Lett 319:133–139. https://doi.org/10.1111/j.1574-6968.2011.02280.x.

31. López-García SL, Perticari A, Piccinetti C, Ventimiglia L, Arias N, De Battista J, Althabegoiti MJ, Mongiardini EJ, Pérez-Giménez J, Quelas JI, Lodeiro AR. 2009. In-furrow inoculation and selection for higher motility enhances the efficacy of *Bradyrhizobium japonicum* nodulation. Agron J 101:1–7. https://doi.org/10.1016/S0065-2113(08)00801-8.

32. Leonard S, Ferooz J, Haine V, Danese I, Fretin D, Tibor A, de Walque S, De Bolle X, Letesson JJ. 2007. FtcR is a new master regulator of the flagellar system of *Brucella melitensis* 16M with homologs in *Rhizobiaceae*. J Bacteriol 189:131–141. https://doi.org/10.1128/JB.00712-06.

33. Kaneko T, Nakamura Y, Sato S, Minamisawa K, Uchiumi T, Sasamoto S, Watanabe A, Idesawa K, Iriguchi M, Kawashima K, Kohara M, Matsumoto M, Shimpo S, Tsuruoka H, Wada T, Yamada M, Tabata S. 2002. Complete genomic sequence of nitrogen-fixing symbiotic bacterium *Bradyrhizobium japonicum* USDA110. DNA Res 9:189–197. https://doi.org/10.1093/dnares/9.6.189.

34. Čuklina J, Hahn J, Imakaev M, Omasits U, Förstner KU, Ljubimov N, Goebel M, Pessi G, Fischer HM, Ahrens CH, Gelfand MS, Evguenieva-Hackenberg E. 2016. Genome-wide transcription start site mapping of *Bradyrhizobium japonicum* grown free-living or in symbiosis: a rich resource to identify new

transcripts, proteins and to study gene regulation. BMC Genomics 17:302. https://doi.org/10.1186/s12864-016-2602-9.

35. Redondo-Nieto M, Lloret J, Larenas J, Barahona E, Navazo A, Martínez-Granero F, Capdevila S, Rivilla R, Martín M. 2008. Transcriptional organization of the region encoding the synthesis of the flagellar filament in *Pseudomonas fluorescens*. J Bacteriol 190:4106–4109. https://doi.org/10.1128/JB.00178-08.

36. Bailey TL, Elkan C. 1994. Fitting a mixture model by expectation maximization to discover motifs in biopolymers. Proc Int Conf Intell Syst Mol Biol 2:28–36.

37. Mangan EK, Malakooti J, Caballero A, Anderson P, Ely B, Gober JW. 1999. FlbT couples flagellum assembly to gene expression in *Caulobacter crescentus*. J Bacteriol 181:6160–6170.

38. Ferooz J, Lemaire J, Letesson JJ. 2011. Role of FlbT in flagellin production in *Brucella melitensis*. Microbiology 157:1253–1262. https://doi.org/10.1099/mic.0.044867-0.

39. Anderson PE, Gober JW. 2000. FlbT, the posttranscriptional regulator of flagellin synthesis in *Caulobacter crescentus*, interacts with the 5′ untranslated region of flagellin mRNA. Mol Microbiol 38:41–52. https://doi.org/10.1046/j.1365-2958.2000.02108.x.

40. Lang AS, Beatty JT. 2002. A bacterial signal transduction system controls genetic exchange and motility. J Bacteriol 184:913–918. https://doi.org/10.1128/jb.184.4.913-918.2002.

41. Sourjik V, Muschler P, Scharf B, Schmitt R. 2000. VisN and VisR are global regulators of chemotaxis, flagellar, and motility genes in *Sinorhizobium* (*Rhizobium*) *meliloti*. J Bacteriol 182:782–788. https://doi.org/10.1128/JB.182.3.782-788.2000.

42. Tambalo DD, Del Bel KL, Bustard DE, Greenwood PR, Steedman AE, Hynes MF. 2010. Regulation of flagellar, motility and chemotaxis genes in *Rhizobium leguminosarum* by the VisN/R-Rem cascade. Microbiology 156:1673–1685. https://doi.org/10.1099/mic.0.035386-0.

43. Thorne DW, Burris RH. 1940. Respiratory enzyme systems in symbiotic nitrogen fixation: III. The respiration of *Rhizobium* from legume nodules and laboratory cultures. J Bacteriol 39:187–196.

44. Lindemann A, Moser A, Pessi G, Hauser F, Friberg M, Hennecke H, Fischer HM. 2007. New target genes controlled by the *Bradyrhizobium japonicum* two-component regulatory system RegSR. J Bacteriol 189:8928–8943. https://doi.org/10.1128/JB.01088-07.

45. Ohkama-Ohtsu N, Honma H, Nakagome M, Nagata M, Yamaya-Ito H, Sano Y, Hiraoka N, Ikemi T, Suzuki A, Okazaki S, Minamisawa K, Yokoyama T. 2016. Growth rate of and gene expression in *Bradyrhizobium diazoefficiens* USDA110 due to a mutation in *blr7984*, a TetR family transcriptional regulator gene. Microbes Environ 31:249–259. https://doi.org/10.1264/jsme2.ME16056.

46. Herlihey FA, Moynihan PJ, Clarke AJ. 2014. The essential protein for bacterial flagella formation FlgJ functions as a β-*N*-acetylglucosaminidase. J Biol Chem 289:31029–31042. https://doi.org/10.1074/jbc.M114.603944.

47. Llewellyn M, Dutton RJ, Easter J, O'Donnol D, Gober JW. 2005. The conserved *flaF* gene has a critical role in coupling flagellin translation and assembly in *Caulobacter crescentus*. Mol Microbiol 57:1127–1142. https://doi.org/10.1111/j.1365-2958.2005.04745.x.

48. Sadowsky MJ, Tully RE, Cregan PB, Keyser HH. 1987. Genetic diversity in *Bradyrhizobium japonicum* serogroup 123 and its relation to genotype-specific nodulation of soybean. Appl Environ Microbiol 53:2624–2630.

49. Vincent JM. 1970. A manual for the practical study of the root nodule bacteria. IBP handbook 15. Blackwell Scientific Publications, Oxford, United Kingdom.

50. Regensburger B, Hennecke H. 1983. RNA polymerase from *Rhizobium japonicum*. Arch Microbiol 135:103–109. https://doi.org/10.1007/BF00408017.

51. Sambrook J, Russell D. 2001. Molecular cloning: a laboratory manual, 3rd ed. Cold Spring Harbor Laboratory Press, New York, NY.

52. Sievers F, Wilm A, Dineen DG, Gibson TJ, Karplus K, Li W, Lopez R, McWilliam H, Remmert M, Söding J, Thompson JD, Higgins DG. 2011. Fast, scalable generation of high-quality protein multiple sequence alignments using Clustal Omega. Mol Syst Biol 7:539. https://doi.org/10.1038/msb.2011.75.

53. McWilliam H, Li W, Uludag M, Squizzato S, Park YM, Buso N, Cowley AP, Lopez R. 2013. Analysis tool web services from the EMBL-EBI. Nucleic

Acids Res 41(Web Server issue):W597–W600. https://doi.org/10.1093/nar/gkt376.

54. Taboada B, Ciria R, Martínez-Guerrero CE, Merino E. 2012. ProOpDB: Prokaryotic Operon DataBase. Nucleic Acids Res 40(Database issue):D627–D631. https://doi.org/10.1093/nar/gkr1020.

55. Mao X, Ma Q, Zhou C, Chen X, Zhang H, Yang J, Mao F, Lai W, Xu Y. 2014. DOOR 2.0: presenting operons and their functions through dynamic and integrated views. Nucleic Acids Res 42(Database issue):D654–D659. https://doi.org/10.1093/nar/gkt1048.

56. Dehal PS, Joachimiak MP, Price MN, Bates JT, Baumohl JK, Chivian D, Friedland GD, Huang KH, Keller K, Novichkov PS, Dubchak IL, Alm EJ, Arkin AP. 2010. MicrobesOnline: an integrated portal for comparative and functional genomics. Nucleic Acids Res 38(Database issue):D396–D400. https://doi.org/10.1093/nar/gkp919.

57. Freese NH, Norris DC, Loraine AE. 2016. Integrated genome browser: visual analytics platform for genomics. Bioinformatics 32:2089–2095. https://doi.org/10.1093/bioinformatics/btw069.

58. Ye J, Coulouris G, Zaretskaya I, Cutcutache I, Rozen S, Madden T. 2012. Primer-BLAST: a tool to design target-specific primers for polymerase chain reaction. BMC Bioinformatics 13:134. https://doi.org/10.1186/1471-2105-13-134.

59. Zuker M. 2003. Mfold web server for nucleic acid folding and hybridization prediction. Nucleic Acids Res 31:3406–3415. https://doi.org/10.1093/nar/gkg595.

60. Crooks GE, Hon G, Chandonia JM, Brenner SE. 2004. WebLogo: a sequence logo generator. Genome Res 14:1188–1190. https://doi.org/10.1101/gr.849004.

61. Quelas JI, Mongiardini EJ, Casabuono A, López-García SL, Althabegoiti MJ, Covelli JM, Pérez-Giménez J, Couto A, Lodeiro AR. 2010. Lack of galactose or galacturonic acid in *Bradyrhizobium japonicum* USDA 110 exopolysaccharide leads to different symbiotic responses in soybean. Mol Plant Microbe Interact 23:1592–1604. https://doi.org/10.1094/MPMI-05-10-0122.

62. Kirchner O, Tauch A. 2003. Tools for genetic engineering in the amino acid-producing bacterium *Corynebacterium glutamicum*. J Biotechnol 104:287–299. https://doi.org/10.1016/S0168-1656(03)00148-2.

63. Vieira J, Messing J. 1982. The pUC plasmids, an M13mp7-derived system for insertion mutagenesis and sequencing with synthetic universal primers. Gene 19:259–268. https://doi.org/10.1016/0378-1119(82)90015-4.

64. Schäfer A, Tauch A, Jäger W, Kalinowski J, Thierbach G, Pühler A. 1994. Small mobilizable multipurpose cloning vectors derived from the *Escherichia coli* plasmids pK18 and pK19: selection of defined deletions in the chromosome of *Corynebacterium glutamicum*. Gene 145:69–73. https://doi.org/10.1016/0378-1119(94)90324-7.

65. Link AJ, Phillips D, Church GM. 1997. Methods for generating precise deletions and insertions in the genome of wild-type *Escherichia coli*: application to open reading frame characterization. J Bacteriol 179:6228–6237. https://doi.org/10.1128/jb.179.20.6228-6237.1997.

66. Dombrecht B, Vanderleyden J, Michiels J. 2001. Stable RK2-derived cloning vectors for the analysis of gene expression and gene function in gram-negative bacteria. Mol Plant Microbe Interact 14:426–430. https://doi.org/10.1094/MPMI.2001.14.3.426.

67. Schneider K, Beck CF. 1987. New expression vectors for identifying and testing signal structures for initiation and termination of transcription. Methods Enzymol 153:452–461. https://doi.org/10.1016/0076-6879(87)53071-3.

68. Hauser F, Lindemann A, Vuilleumier S, Patrignani A, Schlapbach R, Fischer H-M, Hennecke H. 2006. Design and validation of a partial-genome microarray for transcriptional profiling of the *Bradyrhizobium japonicum* symbiotic gene region. Mol Genet Genomics 275:55–67. https://doi.org/10.1007/s00438-005-0059-7.

69. Laemmli UK. 1970. Cleavage of structural proteins during the assembly of the head of bacteriophage T4. Nature 227:680–685. https://doi.org/10.1038/227680a0.

70. Pérez-Giménez J, Covelli JM, López MF, Althabegoiti MJ, Ferrer-Navarro M, Mongiardini EJ, Lodeiro AR. 2012. Soybean seed lectin prevents the accumulation of *S*-adenosyl methionine synthetase and the S1 30S ribosomal protein in *Bradyrhizobium japonicum* under C and N starvation. Curr Microbiol 65:465–474. https://doi.org/10.1007/s00284-012-0180-x.